

Solving the muon $g-2$ anomaly in deflected AMSB with messenger-matter interactions

Fei Wang,^a Wenyu Wang,^b Jin Min Yang^{c,d}

^a*School of Physics, Zhengzhou University, Zhengzhou 450000, P. R. China*

^b*College of Applied Science, Beijing University of Technology, Beijing 100124, P. R. China*

^c*CAS Key Laboratory of Theoretical Physics, Institute of Theoretical Physics, Chinese Academy of Sciences, Beijing 100190, P. R. China*

^d*School of Physics, University of Chinese Academy of Sciences, Beijing 100049, P. R. China*

E-mail: feiwang@zzu.edu.cn, wywang@mail.itp.ac.cn, jmyang@itp.ac.cn

ABSTRACT: General messenger-matter interactions with complete or incomplete GUT multiplet messengers are introduced in the deflected anomaly mediated SUSY breaking scenario to explain the muon $g-2$ anomaly. We find that while the muon $g-2$ anomaly can be solved in both scenarios under current constraints including the LHC bounds on gluino mass, the scenarios with incomplete GUT multiplet messengers are more favored. At the same time, we find that the gluino mass is upper bounded by about 2.5 TeV (2.0 TeV) in Scenario-A and 3.0 TeV (2.7 TeV) in Scenario-B if the generalized deflected AMSB scenarios are used to fully account for the $g-2$ anomaly at 3σ (2σ) level. Such a gluino should be accessible in future LHC searches.

Contents

1	Introduction	2
2	General matter-messenger interactions in deflected AMSB	3
2.1	Two scenarios with messenger-matter interactions	5
2.2	The soft SUSY spectrum in two scenarios	6
3	Solving the muon $g-2$ anomaly in our scenario	11
4	Conclusions	18

1 Introduction

Low energy supersymmetry (SUSY) is strongly motivated and regarded as one of the most appealing candidates for TeV-scale new physics beyond the Standard Model (SM). SUSY can not only solve the gauge hierarchy problem of the SM, but also elegantly explain the cosmic dark matter puzzle. Besides, the gauge coupling unification, which can not be achieved in the SM, can be successfully realized in the framework of SUSY. Especially, the 125 GeV Higgs boson discovered by the LHC [1, 2] lies miraculously in the narrow range of 115 – 135 GeV predicted by the Minimal Supersymmetric Standard Model (MSSM).

Although SUSY is an appealing extension of the SM, currently it seems to have some tensions with the LHC data. In particular, no evidences of SUSY partners (sparticles) have been observed at the LHC. Actually, the LHC data has already set stringent constraints on sparticle masses [3, 4] in simplified SUSY models, e.g., the gluino mass $m_{\tilde{g}} \gtrsim 1.9$ TeV for a massless lightest sparticle (LSP), the lightest stop mass $m_{t_1} \gtrsim 850$ GeV and even stronger bounds on the first two generations of squarks. In fact, the LHC data agrees quite well with the SM predictions and also no significant deviations have been observed in flavor physics or electroweak precision measurements. So far the only sizable deviation comes from the so-called anomalous magnetic moment of the muon $a_\mu = (g_\mu - 2)/2$ measured by the E821 experiment at the Brookhaven National Laboratory [5], which shows a 3.2σ discrepancy from the SM. The SUSY explanation of this anomaly requires relatively light sleptons and electroweak gauginos. If SUSY is indeed the new physics to satisfy or explain all these data, its spectrum must display an intricate structure. Therefore, the origin of SUSY breaking and its mediation mechanism, which determines the low energy SUSY spectrum, is a crucial issue.

There are many popular ways to mediate the SUSY breaking effects from the hidden sector to the visible MSSM sector, such as the anomaly mediation [8], the gravity mediation [6] and the gauge mediation [7]. The anomaly mediated SUSY breaking (AMSB) mechanism predicts a flavour conservation sparticle spectrum. Such a spectrum is insensitive to any high energy theories [9] and thus automatically solves the SUSY flavor problem. Unfortunately, the AMSB scenario predicts tachyonic sleptons so that the minimal theory must be extended. There are several ways to tackle such a tachyonic slepton problem [10]. A very elegant solution is the deflected AMSB [11] scenario, in which additional messenger sectors are introduced to deflect the Renormalization Group Equation (RGE) trajectory and give new contributions to soft SUSY breaking terms. On the other hand, a relatively large number of messenger species are always needed to give positive slepton masses with small negative deflection parameters. However, too many messenger fields may lead to strong gauge couplings below GUT scale or Landau pole below Planck scale. So it is preferred to introduce less messenger species to deflect the RGE trajectory and at the same time give positive slepton masses. In our previous work [14] we proposed to solve this problem by introducing general messenger-matter interactions in the deflected AMSB which has advantages in several aspects.

Note that in order to preserve gauge coupling unification, the messenger species are generally fitted into complete representations of the GUT group. However, sometimes it is

economic and well motivated to introduce incomplete representations of GUT group, such as the adjoint messengers in GMSB, which can still guarantee gauge coupling unification [16–18]. Besides, even the introduction of incomplete representations of messengers, which seems to spoil successful gauge coupling unification, can also be natural in AMSB. This is due to the '*decoupling theorem*' in ordinary anomaly mediation scenario which states that the simple messenger threshold (by pure mass term) will not deflect the AMSB trajectory. By assigning different origin for messenger thresholds (determined by moduli VEV or pure mass term), even a complete representation at high energy may seem as '*incomplete*' in AMSB at low energy. Therefore, the messengers in incomplete GUT representations should also be considered in the study of AMSB.

In this work we focus on the explanation of the muon $g - 2$ anomaly. In order to solve the muon $g - 2$ anomaly and at the same time be compatible with the LHC data, a SUSY spectrum with heavy colored sparticles and light non-colored sparticles is needed. We try to realize such a spectrum in the deflected AMSB scenario with general messenger-matter interactions, where the messengers can form complete or incomplete GUT representations. In our scenario, the slepton sector can receive additional contributions from both the messenger-matter interactions and ordinary deflected anomaly mediation to avoid tachyonic slepton masses, while the colored sparticles can be heavy to evade various collider constraints.

This paper is organized as follows. In Sec 2, we study the soft parameters in the deflected AMSB scenarios with different messenger-matter interactions. The explanation of the muon $g - 2$ in our scenarios and the relevant numerical results are presented in Sec 3. Sec 4 contains our conclusions.

2 General matter-messenger interactions in deflected AMSB

It is well known that the ordinary AMSB has the tachyonic slepton problem. Deflected anomaly mediated SUSY breaking scenario which can change the RGE trajectory below the messenger thresholds can elegantly solve such a problem. However, possible strong couplings at the GUT scale or the Landau pole problem may arise with a small negative deflection parameter. Positively deflected AMSB, which may need specific forms of moduli superpotential [12] or strong couplings [13], is more favored. However, our previous study indicated that the Landau pole problem may still persist with a small positive deflection parameter in order to solve the $g_\mu - 2$ anomaly.

In [14] we proposed to introduce general messenger-matter interactions in the messenger sector which can have several advantages. In this work, the scenarios with complete or incomplete GUT representation messengers accompanied by messenger-matter interactions will be studied. In the second scenario, the incomplete SU(5) GUT representation of messengers are introduced. Note that, the introduction of both adjoint messengers in **3** and **8** representations of SU(2) and SU(3) respectively will not spoil the gauge coupling unification.

Besides, even if the low energy messenger sector seems to spoil the gauge coupling unification, the UV theory can still be consistent with the GUT requirement. As noted previ-

ously, the decoupling theorem in anomaly mediation ensures that the vector-like thresholds with pure mass terms $M_T > M_{mess}$ will not affect the AMSB trajectory upon messenger scales. So each low energy (deflected) AMSB theory with incomplete GUT multiplet messengers below messenger scale M_{mess} could be UV completed to a high energy theory with completed GUT multiplets at certain scale upon M_{mess} . Incomplete GUT multiplet messengers can also origin from orbifold GUT models by proper boundary conditions.

The formulas in deflected AMSB with messenger-matter interactions can be obtained from the wavefunction renormalization approach[15] with superfield wavefunction

$$\begin{aligned} \mathcal{Z}(\tilde{\mu}; \tilde{X}, \tilde{X}^\dagger) &= Z(\mu; X, X^\dagger) + \left[\theta^2 F \frac{\partial}{\partial X} + \bar{\theta}^2 F^\dagger \frac{\partial}{\partial X^\dagger} + (\theta^2 \tilde{F} + \bar{\theta}^2 \tilde{F}^\dagger) \frac{\partial}{\partial \mu} \right] Z(\mu; X, X^\dagger) \\ &+ \theta^2 \bar{\theta}^2 \left(F^\dagger F \frac{\partial^2}{\partial X \partial X^\dagger} + F^\dagger \tilde{F} \frac{\partial^2}{\partial X^\dagger \partial \mu} + \tilde{F}^\dagger F \frac{\partial^2}{\partial X \partial \mu} + \tilde{F}^\dagger \tilde{F} \frac{\partial^2}{\partial \mu^2} \right) Z(\mu; X, X^\dagger). \end{aligned}$$

After canonically normalize the field

$$Q' \equiv Z^{1/2} \left[1 + \theta^2 \left(\frac{F}{M} \frac{\partial}{\partial \ln X} + \frac{\tilde{F}}{\mu} \frac{\partial}{\partial \ln \mu} \right) \ln Z(\mu; X, X^\dagger) \right], \quad (2.1)$$

we can obtain the sfermion masses for the most general forms of deflected AMSB

$$\begin{aligned} m^2 = - \left[\left(\frac{F}{M} \right)^2 \frac{\partial^2}{\partial \ln X^\dagger \partial \ln X} + \left(\frac{\tilde{F}}{\mu} \right)^2 \frac{\partial^2}{\partial \ln \mu^2} \right. \\ \left. + \frac{F \tilde{F}}{M \mu} \left(\frac{\partial^2}{\partial \ln X^\dagger \partial \ln \mu} + \frac{\partial^2}{\partial \ln X \partial \ln \mu} \right) \right] \ln Z(\mu; X, X^\dagger). \quad (2.2) \end{aligned}$$

From the canonicalized normalized superpotential

$$\mathcal{L} = \int d^2\theta \sum_{i=a,b,c} \left[1 - \theta^2 \left(F \frac{\partial}{\partial X} + \tilde{F} \frac{\partial}{\partial \mu} \right) \ln Z(\mu; X, X^\dagger) \right] \left(Z^{-1/2} Q'_i \right) \frac{\partial W [(Z^{-1/2} Q'_i)]}{\partial (Z^{-1/2} Q'_i)},$$

we can obtain the trilinear soft terms

$$\frac{A_{abc}}{y_{abc}} = \sum_{i=a,b,c} \left(\frac{F}{M} \frac{\partial}{\partial X} + \frac{\tilde{F}}{\mu} \frac{\partial}{\partial \mu} \right) \ln Z_i(\mu; X, X^\dagger). \quad (2.3)$$

In our scenario, we have the following replacement

$$\frac{F}{M} \rightarrow dF_\phi, \quad \frac{\tilde{F}}{\mu} \rightarrow -F_\phi/2. \quad (2.4)$$

Details on general messenger-matter interactions in deflected AMSB can be found in our previous work [14].

2.1 Two scenarios with messenger-matter interactions

- Scenario A: deflected AMSB with complete SU(5) GUT representations messengers.

We introduce the following $'N'$ family of new messengers which are fitted into $\mathbf{5}$ and $\bar{\mathbf{5}}$ representation of SU(5) GUT group to deflect the AMSB trajectory

$$\bar{Q}_\phi^I(1, 2)_{1/2}, \quad \tilde{Q}_\phi^I(1, \bar{2})_{-1/2}, \quad \bar{T}_\phi^I(\bar{3}, 1)_{1/3}, \quad T_\phi^I(3, 1)_{-1/3}, \quad (I = 1, \dots, N)$$

We introduce the following superpotential that involves messenger-MSSM-MSSM interaction, typically the slepton-slepton-messenger interaction:

$$W = \sum_I \left(\lambda_A S \bar{Q}_\phi^I \tilde{Q}_\phi^I + \lambda_B S \bar{T}_\phi^I T_\phi^I \right) + \lambda_X S \bar{Q}_\phi^A \tilde{H}_d + W(S) \\ + \sum_{i,j} \left[\tilde{y}_{ij}^E L_{L,i} \tilde{Q}_\phi^A E_{L,j}^c + \tilde{y}_{ij}^D Q_{L,i} \tilde{H}_d D_{L,j}^c + y_{ij}^U Q_{L,i} H_u U_{L,j}^c \right], \quad (2.5)$$

with certain form of superpotential $W(S)$ for pseudo-moduli field S to determine the deflection parameter d . From the form of the interaction, we can see that the slepton soft SUSY breaking parameters will be different from the ordinary deflected AMSB results.

- Scenario B: deflected AMSB with incomplete SU(5) GUT representations messengers.

Motivated by the GMSB with adjoint messenger scenario, we introduce the following incomplete SU(5) GUT representation messengers to deflect the AMSB trajectory

$$\Sigma_O^I(8, 1)_0, \quad \sigma_T^I(1, 3), \quad Z^J(1, 1)_1, \quad \bar{Z}^J(1, 1)_{-1}, \quad I, J = (1, \dots, M); \\ \bar{Q}_\phi^A(1, 2)_{1/2}, \quad \tilde{Q}_\phi^A(1, \bar{2})_{-1/2}, \quad \bar{T}_\phi^A(\bar{3}, 1)_{1/3}, \quad T_\phi^A(3, 1)_{-1/3}.$$

We note that additional singlet messengers Z^I with non-trivial $U(1)_Y$ quantum number can be introduced to deflect the \tilde{E}_L^c slepton RGE trajectory. As in the previous scenario, the superpotential also involves messenger-MSSM-MSSM interaction, typically the slepton-slepton-messenger interaction:

$$W = \lambda_A S \bar{Q}_\phi^A \tilde{Q}_\phi^A + \lambda_B S \bar{T}_\phi^A T_\phi^A + \sum_I \left[\lambda_O S \text{Tr}(\Sigma_O^I \Sigma_O^I) + \lambda_T S \text{Tr}(\Sigma_T^I \Sigma_T^I) \right. \\ \left. + \lambda_Z S \bar{Z}^I Z^I \right] + \lambda_X S \bar{Q}_\phi^A \tilde{H}_d + \sum_{i,j} \left[\tilde{y}_{ij}^E L_{L,i} \tilde{Q}_\phi^A E_{L,j}^c + \tilde{y}_{ij}^D Q_{L,i} \tilde{H}_d D_{L,j}^c \right. \\ \left. + y_{ij}^U Q_{L,i} H_u U_{L,j}^c \right] + W(S) \quad (2.6)$$

We can see that there will be mixing between the messenger \tilde{Q}_ϕ^A and \tilde{H}_d (as well as Q_ϕ^B and H_u). We will define the new states

$$Q_\phi^A \equiv \frac{\lambda_A \tilde{Q}_\phi^A + \lambda_X \tilde{H}_d}{\sqrt{\lambda_A^2 + \lambda_X^2}}, \quad H_d \equiv \frac{-\lambda_X \tilde{Q}_\phi^A + \lambda_A \tilde{H}_d}{\sqrt{\lambda_A^2 + \lambda_X^2}}. \quad (2.7)$$

After the substitution of the new states, the superpotential changes to

$$\begin{aligned}
W = & \sqrt{\lambda_A^2 + \lambda_X^2} S \bar{Q}_\phi^A Q_\phi^A + \sum_{i,j} y_{ij}^U Q_{L,i} H_u U_{L,j}^c + \sum_{F_H=T_\phi^I, Q_\phi^I, \dots} \lambda_{F_H} S \bar{F}_H F_H + W(S) \\
& + \sum_{i,j} \tilde{y}_{ij}^E L_{L,i} \frac{\lambda_A Q_\phi^A - \lambda_X H_d}{\sqrt{\lambda_A^2 + \lambda_X^2}} E_{L,j}^c + \tilde{y}_{ij}^D Q_{L,i} \frac{\lambda_X Q_\phi^A + \lambda_A H_d}{\sqrt{\lambda_A^2 + \lambda_X^2}} D_{L,j}^c, \quad (2.8)
\end{aligned}$$

We have the following relation

$$\tilde{y}_{ij}^E \frac{\lambda_X}{\sqrt{\lambda_A^2 + \lambda_X^2}} = y_{ij}^E, \quad -\tilde{y}_{ij}^D \frac{\lambda_A}{\sqrt{\lambda_A^2 + \lambda_X^2}} = y_{ij}^D. \quad (2.9)$$

We define

$$\tilde{y}_{ij}^E \frac{\lambda_A}{\sqrt{\lambda_A^2 + \lambda_X^2}} \equiv -\lambda_{ij}^E, \quad -\tilde{y}_{ij}^D \frac{\lambda_X}{\sqrt{\lambda_A^2 + \lambda_X^2}} \equiv \lambda_{ij}^D, \quad \sqrt{\lambda_A^2 + \lambda_X^2} \equiv \lambda_S. \quad (2.10)$$

So the superpotential can be rewritten as

$$\begin{aligned}
W = & \lambda_S S \bar{Q}_\phi^A Q_\phi^A + \sum_{i,j} y_{ij}^U Q_{L,i} H_u U_{L,j}^c + \sum_{F_H=Z^I, Q^I, \dots} \lambda_{F_H} S \bar{F}_H F_H + W(S) \\
& - \sum_{i,j} [\lambda_{ij}^E L_{L,i} Q_\phi^A E_{L,j}^c + y_{ij}^E L_{L,i} H_d E_{L,j}^c + \lambda_{ij}^D Q_{L,i} Q_\phi^A D_{L,j}^c + y_{ij}^D Q_{L,i} H_d D_{L,j}^c] \quad (2.11)
\end{aligned}$$

For simplicity, we chose $\lambda_{ij}^E = \lambda_E \delta_{ij}$, $\lambda_{ij}^D = \lambda_D \delta_{ij}$ to be diagonal. Below the messenger threshold determined by the VEV of pseudo-moduli S , we can integrate out the heavy fields F_H, Q_ϕ^A and obtain the low energy MSSM.

2.2 The soft SUSY spectrum in two scenarios

From the superpotential, the soft SUSY breaking parameters can be calculated. In the calculation, the wavefunction renormalization approach [19] is used in which messenger threshold M_{mess}^2 is replaced by spurious chiral fields X with $M_{mess}^2 = X^\dagger X$. The most general type of expressions in AMSB can be found in our previous work [14].

We can calculate the change of the gauge beta-function

$$\Delta\beta_{g_i} = \frac{1}{16\pi^2} g_i^3 \Delta b_{g_i}, \quad (2.12)$$

with

$$\Delta(b_3, b_2, b_1) = (N, N, N), \quad (2.13)$$

for Scenario A. For Scenario B we consider two cases. One is

$$\Delta(b_3, b_2, b_1) = (3M + 1, 2M + 1, 1) \quad \text{Scenario B1} \quad (2.14)$$

in which ' $I = M, J = 0$ ' is adopted to guarantee apparently gauge coupling unification. The other is

$$\Delta(b_3, b_2, b_1) = (3M + 1, 2M + 1, \frac{6M}{5} + 1) \quad \text{Scenario B2} \quad (2.15)$$

with ' $I = J = M'$ ' in which apparently the gauge coupling unification is spoiled. However, as we discussed previously, the successful GUT may still be possible if certain additional incomplete messengers upon ' X ' threshold are introduced in the UV completed theory.

From the general expressions in Eq.(2.2), we can see that there are three types of contributions to the soft SUSY breaking parameters:

- The interference contribution part given by

$$\begin{aligned} \delta^I &= \frac{\partial^2}{\partial \ln \mu \partial \ln X} \ln Z_{ab}^D \\ &= \frac{\partial^2}{\partial \ln \mu \partial \ln X} Z^D - \frac{\partial}{\partial \ln \mu} Z^D \frac{\partial}{\partial \ln X} Z^D \\ &= \left(\frac{\Delta G_a^D}{2} \frac{\partial}{\partial Z_a^D} + \frac{\Delta \beta_{g_r}}{2} \frac{\partial}{\partial g_r} \right) G^- - G_a^D \frac{\Delta G_a}{2} . \end{aligned} \quad (2.16)$$

In our convention, the anomalous dimensions are expressed in the holomorphic basis [20, 21]

$$G^i \equiv \frac{dZ_{ij}}{d \ln \mu} \equiv -\frac{1}{8\pi^2} \left(\frac{1}{2} d_{kl}^i \lambda_{ikl}^* \lambda_{jmn} Z_{km}^{-1*} Z_{ln}^{-1*} - 2c_r^i Z_{ij} g_r^2 \right), \quad (2.17)$$

We define ($\Delta G \equiv G^+ - G^-$), the discontinuity across the integrated heavy field threshold with $G^+(G^-)$ denoting the value upon (below) such threshold.

The discontinuities of the relevant couplings are given as

$$\Delta G_{y_t} = -\frac{1}{8\pi^2} (\lambda_D^2), \quad (2.18)$$

$$\Delta G_{y_b} = -\frac{1}{8\pi^2} (3\lambda_D^2), \quad (2.19)$$

$$\Delta G_{y_\tau} = -\frac{1}{8\pi^2} (3\lambda_E^2) \quad (2.20)$$

We take into account the terms involving $y_t, y_b, y_\tau, g_i, \lambda$, and the subleading terms are neglected in the calculation. The new interference contributions from the messenger-matter interactions are given as

$$2\delta_{Q_{L,i}}^I = \delta_{i,3} \frac{dF_\phi^2}{8\pi^2} [y_t^2 \Delta G_{y_t} + y_b^2 \Delta G_{y_b}], \quad (2.21)$$

$$2\delta_{U_{L,i}^c}^I = \delta_{i,3} \frac{dF_\phi^2}{8\pi^2} [2y_t^2 \Delta G_{y_t}], \quad (2.22)$$

$$2\delta_{D_{L,i}^c}^I = \delta_{i,3} \frac{dF_\phi^2}{8\pi^2} [2y_b^2 \Delta G_{y_b}], \quad (2.23)$$

$$2\delta_{L,i}^I = \delta_{i,3} \frac{dF_\phi^2}{8\pi^2} [y_\tau^2 \Delta G_{y_\tau}] , \quad (2.24)$$

$$2\delta_{E,i}^I = \delta_{i,3} \frac{dF_\phi^2}{8\pi^2} [2y_\tau^2 \Delta G_{y_\tau}] , \quad (2.25)$$

$$2\delta_{H_u}^I = \frac{dF_\phi^2}{8\pi^2} [3y_t^2 \Delta G_{y_t}] , \quad (2.26)$$

$$2\delta_{H_d}^I = \frac{dF_\phi^2}{8\pi^2} [3y_b^2 \Delta G_{y_b} + y_\tau^2 \Delta G_{y_\tau}] , \quad (2.27)$$

with $\delta_{i,j}$ the Kronecker delta. Terms involving the gauge parts are absorbed in the deflected AMSB contributions involving G_i .

- The pure gauge mediation part given by

$$\delta^G = \frac{\partial^2}{\partial \ln X \ln X^\dagger} \ln Z^D = \frac{\partial^2}{\partial \ln X \ln X^\dagger} Z^D - \frac{\partial Z^D}{\partial \ln X} \frac{\partial Z^D}{\partial \ln X^\dagger} . \quad (2.28)$$

Note that

$$\Delta G_{Q_i Q_i} = -\frac{1}{8\pi^2} [\lambda_D^2] , \quad (2.29)$$

$$\Delta G_{D_i D_i} = -\frac{1}{8\pi^2} [2\lambda_D^2] , \quad (2.30)$$

$$\Delta G_{E_i E_i} = -\frac{1}{8\pi^2} 2\lambda_E^2 , \quad (2.31)$$

$$\Delta G_{L_i L_i} = -\frac{1}{8\pi^2} \lambda_E^2 , \quad (2.32)$$

and

$$G_{L_i L_i}^+ = -\frac{1}{8\pi^2} [\lambda_E^2 + y_\tau^2 \delta_{i,3}] , \quad (2.33)$$

$$G_{E_i E_i}^+ = -\frac{1}{8\pi^2} 2 [\lambda_E^2 + y_\tau^2 \delta_{i,3}] , \quad (2.34)$$

$$G_{Q_i Q_i}^+ = -\frac{1}{8\pi^2} [\lambda_D^2 + (y_b^2 + y_t^2) \delta_{i,3}] , \quad (2.35)$$

$$G_{D_i D_i}^+ = -\frac{1}{8\pi^2} 2 [\lambda_D^2 + y_b^2 \delta_{i,3}] , \quad (2.36)$$

$$G_{Q_\phi Q_\phi}^+ = -\frac{1}{8\pi^2} [\lambda_E^2 + 3\lambda_D^2 + \lambda_S^2] , \quad (2.37)$$

and also the anomalous dimension above the messenger threshold

$$\begin{aligned} G_{\lambda_{ii}^D}^+ &= G_{Q_i Q_i}^+ + G_{D_i D_i}^+ + G_{Q_\phi Q_\phi}^+ \\ &= -\frac{1}{8\pi^2} \left[6\lambda_D^2 + \lambda_E^2 + \lambda_S^2 + (3y_b^2 + y_t^2) \delta_{i,3} - \frac{16}{3} g_3^2 - 3g_2^2 - \frac{7}{15} g_1^2 \right] , \end{aligned} \quad (2.38)$$

$$\begin{aligned} G_{\lambda_{ii}^E}^+ &= G_{L_i L_i}^+ + G_{E_i E_i}^+ + G_{Q_\phi Q_\phi}^+ \\ &= -\frac{1}{8\pi^2} \left[4\lambda_E^2 + 3\lambda_D^2 + \lambda_S^2 + 3y_\tau^2 \delta_{i,3} - 3g_2^2 - \frac{9}{5} g_1^2 \right] , \end{aligned} \quad (2.39)$$

so we have

$$4\delta_{Q_i}^G = \frac{d^2 F_\phi^2}{8\pi^2} \left[\lambda_D^2 G_{\lambda_{ii}^D}^+ \right] - \frac{d^2 F_\phi^2}{8\pi^2} \delta_{i,3} \left[y_t^2 \Delta G_{y_t} + y_b^2 \Delta G_{y_b} \right] , \quad (2.40)$$

$$4\delta_{D_i}^G = \frac{d^2 F_\phi^2}{8\pi^2} \left[2\lambda_D^2 G_{\lambda_{ii}^D}^+ \right] - \frac{d^2 F_\phi^2}{8\pi^2} \delta_{i,3} \left[2y_b^2 \Delta G_{y_b} \right] , \quad (2.41)$$

$$4\delta_{U_i}^G = -\frac{d^2 F_\phi^2}{8\pi^2} \delta_{i,3} \left[2y_t^2 \Delta G_{y_t} \right] , \quad (2.42)$$

$$4\delta_{L_i}^G = \frac{d^2 F_\phi^2}{8\pi^2} \left[\lambda_E^2 G_{\lambda_{ii}^E}^+ \right] - \frac{d^2 F_\phi^2}{8\pi^2} \delta_{i,3} \left[y_\tau^2 \Delta G_{y_\tau} \right] , \quad (2.43)$$

$$4\delta_{E_i}^G = \frac{d^2 F_\phi^2}{8\pi^2} \left[2\lambda_E^2 G_{\lambda_{ii}^E}^+ \right] - \frac{d^2 F_\phi^2}{8\pi^2} \delta_{i,3} \left[2y_\tau^2 \Delta G_{y_\tau} \right] , \quad (2.44)$$

$$4\delta_{H_u}^G = -\frac{d^2 F_\phi^2}{8\pi^2} \left[3y_t^2 \Delta G_{y_t} \right] , \quad (2.45)$$

$$4\delta_{H_d}^G = -\frac{d^2 F_\phi^2}{8\pi^2} \left[3y_b^2 \Delta G_{y_b} + y_\tau^2 \Delta G_{y_\tau} \right] \quad (2.46)$$

- The pure deflected AMSB contributions without messenger-matter interactions given by

$$\begin{aligned} \delta_A &= \frac{d^2 Z^D}{dt^2} - \left(\frac{dZ^D}{dt} \right)^2 \\ &= \left(G_a^D \frac{\partial}{\partial Z_a} + \beta_g^i \frac{\partial}{\partial g_i} \right) G^D - (G_D^2) , \end{aligned} \quad (2.47)$$

The expressions are given by

$$\begin{aligned} \delta_{\tilde{Q}_{L,i}}^A &= \frac{F_\phi^2}{16\pi^2} \left[\frac{8}{3} G_3 \alpha_3^2 + \frac{3}{2} G_2 \alpha_2^2 + \frac{1}{30} G_1 \alpha_1^2 \right] \\ &\quad + \delta_{3,i} \frac{F_\phi^2}{(16\pi^2)^2} y_t^2 (6y_t^2 + y_b^2 - \frac{16}{3} g_3^2 - 3g_2^2 - \frac{13}{15} g_1^2) \\ &\quad + \delta_{3,i} \frac{F_\phi^2}{(16\pi^2)^2} y_b^2 (y_t^2 + 6y_b^2 + y_\tau^2 - \frac{16}{3} g_3^2 - 3g_2^2 - \frac{7}{15} g_1^2) , \end{aligned} \quad (2.48)$$

$$\begin{aligned} \delta_{\tilde{U}_{L,i}^c}^A &= \frac{F_\phi^2}{16\pi^2} \left[\frac{8}{3} G_3 \alpha_3^2 + \frac{8}{15} G_1 \alpha_1^2 \right] \\ &\quad + \delta_{3,i} \frac{F_\phi^2}{(16\pi^2)^2} 2y_t^2 (6y_t^2 + y_b^2 - \frac{16}{3} g_3^2 - 3g_2^2 - \frac{13}{15} g_1^2) , \end{aligned} \quad (2.49)$$

$$\begin{aligned} \delta_{\tilde{D}_{L,i}^c}^A &= \frac{F_\phi^2}{16\pi^2} \left[\frac{8}{3} G_3 \alpha_3^2 + \frac{2}{15} G_1 \alpha_1^2 \right] \\ &\quad + \delta_{3,i} \frac{F_\phi^2}{(16\pi^2)^2} 2y_b^2 (y_t^2 + 6y_b^2 + y_\tau^2 - \frac{16}{3} g_3^2 - 3g_2^2 - \frac{7}{15} g_1^2) , \end{aligned} \quad (2.50)$$

$$\begin{aligned}\delta_{\tilde{H}_u}^A &= \frac{F_\phi^2}{16\pi^2} \left[\frac{3}{2} G_2 \alpha_2^2 + \frac{3}{10} G_1 \alpha_1^2 \right] \\ &\quad + \frac{F_\phi^2}{(16\pi^2)^2} 3y_t^2 (6y_t^2 + y_b^2 - \frac{16}{3} g_3^2 - 3g_2^2 - \frac{13}{15} g_1^2),\end{aligned}\quad (2.51)$$

$$\begin{aligned}\delta_{\tilde{H}_d}^A &= \frac{F_\phi^2}{16\pi^2} \left[\frac{3}{2} G_2 \alpha_2^2 + \frac{3}{10} G_1 \alpha_1^2 \right] \\ &\quad + \frac{F_\phi^2}{(16\pi^2)^2} 3y_b^2 (y_t^2 + 6y_b^2 + y_\tau^2 - \frac{16}{3} g_3^2 - 3g_2^2 - \frac{7}{15} g_1^2) \\ &\quad + \frac{F_\phi^2}{(16\pi^2)^2} y_\tau^2 \left(4y_\tau^2 + 3y_b^2 - 3g_2^2 - \frac{9}{5} g_1^2 \right),\end{aligned}\quad (2.52)$$

$$\begin{aligned}\delta_{\tilde{L}_{L,i}}^A &= \frac{F_\phi^2}{16\pi^2} \left[\frac{3}{2} G_2 \alpha_2^2 + \frac{3}{10} G_1 \alpha_1^2 \right] \\ &\quad + \delta_{3,i} \frac{F_\phi^2}{(16\pi^2)^2} y_\tau^2 \left(4y_\tau^2 + 3y_b^2 - 3g_2^2 - \frac{9}{5} g_1^2 \right),\end{aligned}\quad (2.53)$$

$$\delta_{\tilde{E}_{L,i}^c}^A = \frac{F_\phi^2}{16\pi^2} \left[\frac{6}{5} G_1 \alpha_1^2 \right] + \delta_{3,i} \frac{F_\phi^2}{(16\pi^2)^2} 2y_\tau^2 \left(4y_\tau^2 + 3y_b^2 - 3g_2^2 - \frac{9}{5} g_1^2 \right), \quad (2.54)$$

with

$$G_i = (\Delta b_i) d^2 + 2(\Delta b_i) d - b_i, \quad (2.55)$$

$$(b_1, b_2, b_3) = \left(\frac{33}{5}, 1, -3 \right). \quad (2.56)$$

So we obtain the final results of soft SUSY breaking parameters for sfermions

$$m_i^2 = -\delta_i^I + \delta_i^G + \delta_i^A, \quad (2.57)$$

with d being the deflection parameter.

The trilinear coupling will also receive new contributions which are given by

$$A_t = \frac{F_\phi}{16\pi^2} \left[6y_t^2 + y_b^2 - (\lambda_D^2) d - \frac{16}{3} g_3^2 - 3g_2^2 - \frac{13}{15} g_1^2 \right], \quad (2.58)$$

$$A_b = \frac{F_\phi}{16\pi^2} \left[y_t^2 + 6y_b^2 + y_\tau^2 - (3\lambda_D^2) d - \frac{16}{3} g_3^2 - 3g_2^2 - \frac{7}{15} g_1^2 \right], \quad (2.59)$$

$$A_\tau = \frac{F_\phi}{16\pi^2} \left[4y_\tau^2 + 3y_b^2 - (3\lambda_E^2) d - 3g_2^2 - \frac{9}{5} g_1^2 \right]. \quad (2.60)$$

while for the first two generations they are given by

$$A_U = \frac{F_\phi}{16\pi^2} \left[-(\lambda_D^2) d - \frac{16}{3} g_3^2 - 3g_2^2 - \frac{13}{15} g_1^2 \right], \quad (2.61)$$

$$A_D = \frac{F_\phi}{16\pi^2} \left[-(3\lambda_D^2) d - \frac{16}{3} g_3^2 - 3g_2^2 - \frac{7}{15} g_1^2 \right], \quad (2.62)$$

$$A_E = \frac{F_\phi}{16\pi^2} \left[-(3\lambda_E^2)d - 3g_2^2 - \frac{9}{5}g_1^2 \right]. \quad (2.63)$$

The gaugino masses are determined by

$$\begin{aligned} m_{\lambda_i} &= g^2 \frac{F_\phi}{2} \left(\frac{\partial}{\partial \ln \mu} - d \frac{\partial}{\partial \ln |X|} \right) \frac{1}{g^2(\mu, X)} \\ &= g^2 \frac{F_\phi}{2} \left(2 \frac{1}{16\pi^2} b_i - 2d \frac{1}{16\pi^2} \Delta b_i \right) \\ &= g^2 \frac{F_\phi}{16\pi^2} (b_i - d\Delta b_i). \end{aligned} \quad (2.64)$$

So we have

$$m_{\lambda_i} = \frac{F_\phi}{4\pi} \alpha_i (b_i - d\Delta b_i). \quad (2.65)$$

Therefore, the gaugino masses at the messenger scale are given as

$$M_3 = \frac{F_\phi}{4\pi} \alpha_3 [-3 - d(\Delta b_3)] , \quad (2.66)$$

$$M_2 = \frac{F_\phi}{4\pi} \alpha_2 [1 - d(\Delta b_2)] , \quad (2.67)$$

$$M_1 = \frac{F_\phi}{4\pi} \alpha_1 [6.6 - d(\Delta b_1)] . \quad (2.68)$$

It is well known in AMSB that naively adding a supersymmetric μ term to the Lagrangian will lead to unrealistic large $B\mu = \mu F_\phi$. So the generations of μ and B_μ in AMSB may have a different origin and are model dependent. In fact, there are already many proposals to generate realistic μ and $B\mu$, for example, by promoting to NMSSM [22] or introducing a new singlet [23]. We will treat them as free parameters in this scenario.

3 Solving the muon $g-2$ anomaly in our scenario

The E821 experimental result of the muon anomalous magnetic moment at the Brookhaven AGS [5]

$$a_\mu^{\text{expt}} = 116592089(63) \times 10^{-11} , \quad (3.1)$$

is larger than the SM prediction

$$a_\mu^{\text{SM}} = 116591834(49) \times 10^{-11} . \quad (3.2)$$

The deviation is about 3.2σ

$$\Delta a_\mu(\text{expt} - \text{SM}) = (255 \pm 80) \times 10^{-11}. \quad (3.3)$$

SUSY can yield sizable contributions to the muon $g-2$ which dominantly come from the chargino-sneutrino and the neutralino-smuon loop diagrams. The muon $g-2$ anomaly,

which is order 10^{-9} , can be explained for $m_{\text{SUSY}} = \mathcal{O}(100)$ GeV and $\tan\beta = \mathcal{O}(10)$. In our scenario, slepton masses as well as M_1, M_2 can be relatively light. On the other hand, the colored sparticles can be heavy to evade possible constraints from the LHC, the SUSY flavor and CP problems.

The soft terms are characterized by the following free parameters at the messenger scale

$$d, M_{\text{mess}}, F_\phi, \tan\beta, \lambda^D, \lambda^E, \lambda_S, \lambda_{F_H} \quad (3.4)$$

All the inputs should be seen as the boundary conditions at the messenger scale, which after RGE running to the EW scale, could give the low energy spectrum. About these parameters we have the following comments:

- The value of F_ϕ is chosen to lie in the range $1\text{TeV} < F_\phi < 500\text{TeV}$. We know that the value of F_ϕ determines the whole spectrum. On the one hand, F_ϕ cannot be very low due to the constraints from the gaugino masses. On the other hand, a very heavy F_ϕ will spoil the EWSB requirement and give a Higgs mass heavier than the LHC results.
- The messenger scale M_{mess} can be chosen to be less than the GUT scale and at the same time heavier than the sparticle spectrum. So we choose $1\text{TeV} \leq M_{\text{mess}} \leq 10^{15}\text{GeV}$.
- We choose the deflection parameter in the range $-5 \leq d \leq 5$ and $\tan\beta$ in the range $2 \leq \tan\beta \leq 50$.
- The parameters $\lambda_D, \lambda_E, \dots$ can be chosen in the range $0 < |\lambda| < \sqrt{4\pi}$ which ensure positive contributions to slepton masses regardless of the (sign of) deflection parameter d . This is the advantage of our scenario which needs less messenger species with a given d .

We also take into account the following collider and dark matter constraints:

- (1) The mass range for the Higgs boson $123\text{GeV} < M_h < 127\text{GeV}$ from ATLAS and CMS [1, 2].
- (2) The lower bounds on neutralino and charginos masses, including the invisible decay bounds for Z -boson [24].
- (3) The dark matter relic density from the Planck result $\Omega_{DM} = 0.1199 \pm 0.0027$ [25] (in combination with the WMAP data [26]) and the limits of the LUX-2016[27], the PandaX[28] spin-independent dark matter scattering cross section .
- (4) Flavor constraints from the rare decays of B-mesons. For $B_S \rightarrow X_s \gamma$ we use the recent experimental results [29]

$$2.99 \times 10^{-4} < Br(B_S \rightarrow X_s \gamma) < 3.87 \times 10^{-4} . \quad (3.5)$$

(5) The electroweak precision observables [30], such as

$$\delta M_W^{\text{exp}} \approx \pm 30 \text{ MeV}, \quad \delta \sin \theta_{\text{eff}}^{\text{exp}} \approx \pm 15 \times 10^{-5}. \quad (3.6)$$

(6) Current LHC constraints on sparticle masses [31]:

- Gluino mass $m_{\tilde{g}} \gtrsim 1.5 \sim 1.9 \text{ TeV}$;
- Light stop mass $m_{\tilde{t}_1} \gtrsim 0.85 \text{ TeV}$;
- Light sbottom mass $m_{\tilde{b}_1} \gtrsim 0.84 \text{ TeV}$;
- First two generation squarks $m_{\tilde{q}} \gtrsim 1.0 \sim 1.4 \text{ TeV}$.

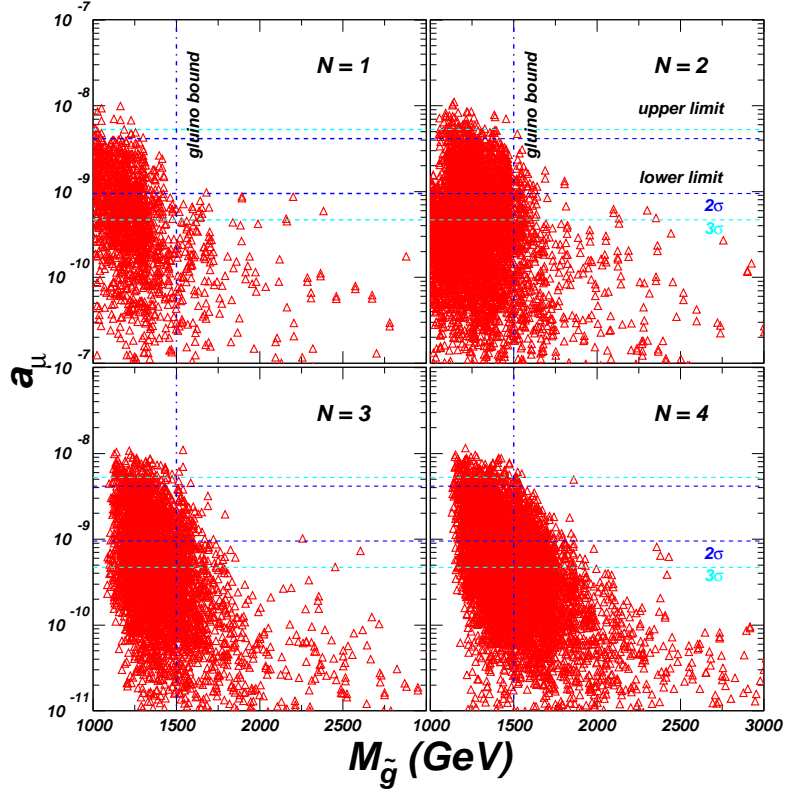


Figure 1. The scatter plots of the survived samples showing the muon $g-2$ versus the gluino mass in Scenario A with complete GUT multiplets. The blue (cyan) dash line indicate the 2σ (3σ) range of the $g-2$ data. A gluino lower bound $m_{\tilde{g}} \gtrsim 1.5 \text{ TeV}$ is shown in the figure.

From the numerical results, we have the following observations:

- Scenario A: Fig.1 shows the scan results of Scenario A in which the Δa_μ versus $m_{\tilde{g}}$ plots with complete GUT multiplets are given. The blue (cyan) dashed line indicate the 2σ (3σ) range of $g_\mu - 2$ data. All survived points satisfy the constraints (1-6) except the bounds from the dark matter relic density and the gluino mass. The most stringent constraints come from the LHC bounds on gluino mass, which excluded a great majority of the survived points that solve the $g_\mu - 2$ anomaly at 2σ level. As

the messenger species number N gets larger, more and more points can survive the gluino mass bound.

The gluino is upper bounded by about 2.5 TeV (2.0 TeV) if the $g_\mu - 2$ anomaly is solved at 3σ (2σ) level. We know that the $g_\mu - 2$ anomaly can be solved if the relevant sparticles $\tilde{\mu}, \tilde{\nu}_\mu, \tilde{B}_\mu, \tilde{W}_\mu$ are lighter than $600 \sim 700$ GeV [5] (the region with a smaller $\tan\beta$ needs even lighter sparticles). In AMSB, the whole low energy spectrum is determined by the value of F_ϕ . So, in order to solve the $g_\mu - 2$ anomaly, the mass scale of $\tilde{\mu}, \tilde{\nu}_\mu, \tilde{B}_\mu, \tilde{W}_\mu$ determines the upper bound of F_ϕ , which, on the other hand, sets a bound on gluino mass. The allowed range of F_ϕ versus the messenger scale M_{mess} in Scenario A is shown in the left panel of Fig 2. It is obvious from the plots that the scale of F_ϕ is indeed upper bounded to account for the $g_\mu - 2$ anomaly. We should note that the deflection of the RGE trajectory and the messenger-matter interactions can loosen the bound of F_ϕ in comparison with the ordinary AMSB.

The deflection parameter d versus the messenger-matter couplings $\lambda_E \equiv \lambda$ is plotted in the right panel of Fig 2. We see that additional messenger-matter interactions are welcome to explain the $g_\mu - 2$ anomaly. Only a small range of d is allowed without leptonic messenger-matter interactions ($\lambda_E = 0$). However, the allowed range for d enlarges with non-trivial messenger-matter interactions.

Our numerical results indicate that the majority part of the allowed parameter space can not satisfy the the upper bound of dark matter relic density. This result can be understood from the hierarchies among the gauginos at the EW scale. From Eq.(2.65), the gaugino mass ratios at the weak scale are given by

$$M_1 : M_2 : M_3 \approx [6.6 - d(\Delta b_1)] : 2[1 - d(\Delta b_2)] : 6[-3 - d(\Delta b_3)] . \quad (3.7)$$

Knowing the range of the deflection parameter d , the lightest gaugino can be identified. It can be seen in case $N = 1$ that the deflection parameter d is lower bounded to $d \gtrsim 1.5$ for a positive d while $d \lesssim -4.5$ for a negative d . From Eq.(3.7) we can see that for $-4.6 < d < 2.8$ the lightest gaugino will be the wino, otherwise the lightest gaugino will be the bino. The dark matter relic density constraint for a bino-like LSP is very stringent. So in a majority of the parameter space allowed by $g_\mu - 2$ and gluino mass bound, the LSP will be bino-like and can not give the right DM relic density. On the other hand, a small portion of the allowed parameter space will predict a wino-like LSP which will lead to insufficient dark matter abundance for a wino mass below 3 TeV. Heavy wino-like LSP of order 3 TeV will always lead to heavy bino and sleptons which otherwise can not explain the $g_\mu - 2$ anomaly. Given the upper bounds on F_ϕ from $g_\mu - 2$ and gluino mass, the wino will always be much lighter than 3 TeV. We give in Table 1 the range of d , within which the wino will be lighter than bino for various messenger species N . We can see that only a small portion of parameter space with a positive d can easily satisfy the dark matter relic density upper bound. The vast parameter space with a bino-like LSP will be stringently constrained by dark matter relic density upper bound. We checked that only a very small region

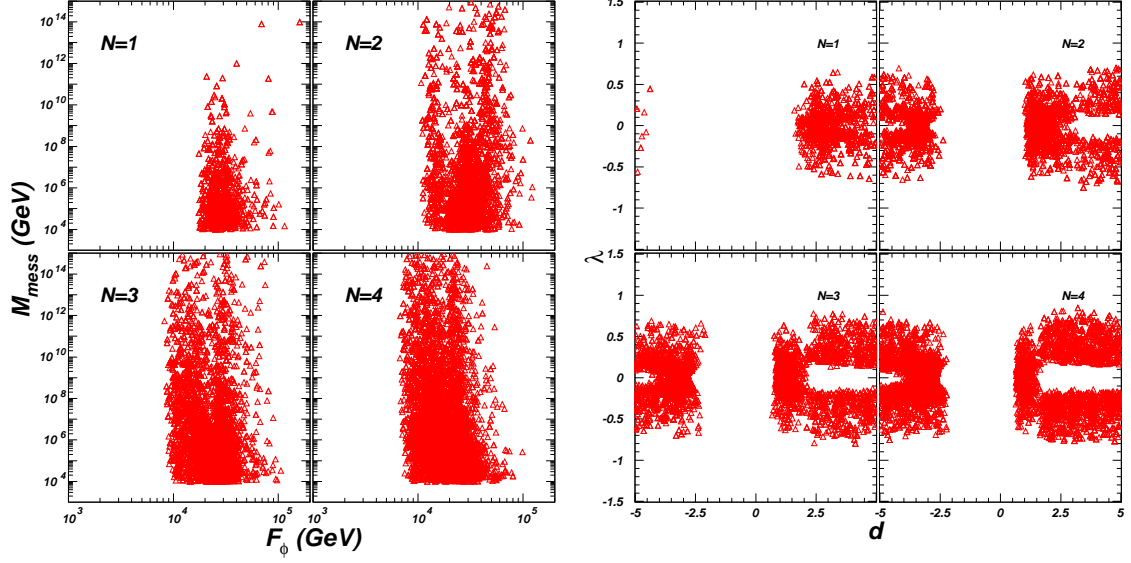


Figure 2. Same as Fig.1, but showing the value of F_ϕ versus the messenger scale M_{mess} (the left panel) and the deflection parameter d versus the messenger-matter couplings $\lambda \equiv \lambda_E$ (the right panel).

can satisfy such relic density constraints. So generalized deflected AMSB scenarios with complete GUT representation of messengers are not favored in solving the $g_\mu - 2$ discrepancy.

Table 1. The range of d within which the wino will be lighter than bino for various messenger species N in Scenario A.

	N=1	N=2	N=3	N=4
d	$-4.6 < d < 2.86$	$-2.3 < d < 1.43$	$-1.53 < d < 0.95$	$-1.15 < d < 0.72$

We should note that the constraints from the gluino can be alleviated if we introduce pure colored messenger particles (without $SU(2)_L$ and $U(1)_Y$ quantum numbers). We can see from the expressions for the soft SUSY parameters that the value of Δb_3 can essentially control the gluino mass. More pure colored messenger particles always mean a heavy gluino for a positive deflection parameter which, on the other hand, may spoil the gauge coupling unification. As noted in the previous section, the complete representation messengers may seem '*incomplete*' at the low energy X threshold. However, the perturbative gauge coupling unification may be spoiled with more additional messenger species. We will discuss the detailed consequence of general messenger sectors versus gauge coupling unification in our subsequent studies.

- Scenario B:

The scatter plots of the survived samples showing a_μ versus $m_{\tilde{g}}$ in Scenario B are shown in Fig.3, in which the upper panel is for Scenario B1 and the lower panel is for Scenario B2. We can see that a lot of points which can fully account for the $g_\mu - 2$ anomaly can survive the LHC gluino mass bound, especially, for a larger M .

So scenarios with the incomplete GUT representation of messengers is more favored by the $g_\mu - 2$ data.

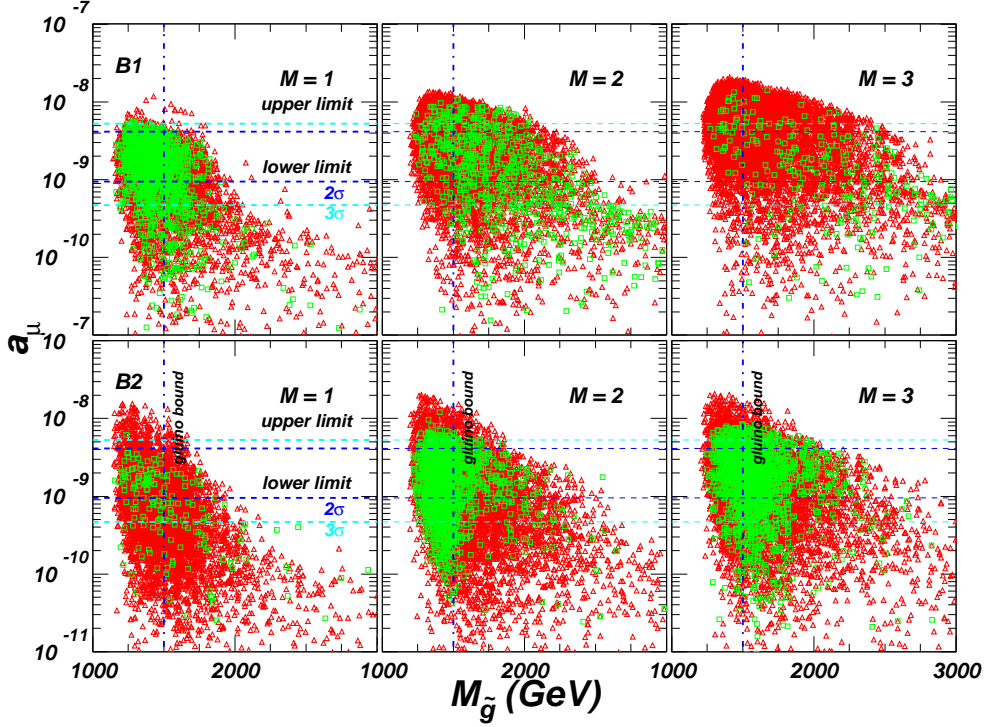


Figure 3. The scatter plots of the survived samples showing the muon $g - 2$ versus the gluino mass in Scenario B with incomplete GUT multiplets (adjoint messengers). The upper panel corresponds to Scenario B1 while the lower panel is for Scenario B2. The green ' \square ' samples satisfy both the upper and lower bounds of the dark matter relic density.

Similar to Scenario A, the upper bound of gluino mass can be understood from the upper bound of F_ϕ , which is obvious in Fig.4 for both cases. The upper mass bound of gluino is around 3 TeV (2.7 TeV) in both scenarios if the muon $g - 2$ is explained at 3σ (2σ) level. Such a light gluino will be accessible at future LHC experiments.

The deflection parameter d versus the messenger-matter couplings $\lambda_E \equiv \lambda$ in Scenario B is plotted in Fig.5 with all points satisfying both the upper and lower bound of DM relic density. Again, additional non-trivial messenger-matter interactions are obviously advantageous in solving the $g_\mu - 2$ anomaly with which the allowed range for d enlarges. Besides, the non-vanishing messenger-matter interactions $\lambda \neq 0$ can be used to solved the $g_\mu - 2$ anomaly for a relatively small deflection parameter d , especially for the Scenario B1. We can see from Fig.5 that in Scenario B1 the maximum negative d is -3.5 with $\lambda = 0$. However, the maximum negative d changes to almost -2 with non-vanishing messenger-matter interactions. A small deflection parameter $|d|$ is relatively easy for model buildings. In Scenario B2, it is not possible to solve the $g_\mu - 2$ anomaly with $\lambda = 0$ for a positive d . With messenger-matter interactions, a positive deflection parameter also works.

In Fig.5 the survived points which satisfy both the upper and lower bounds of dark

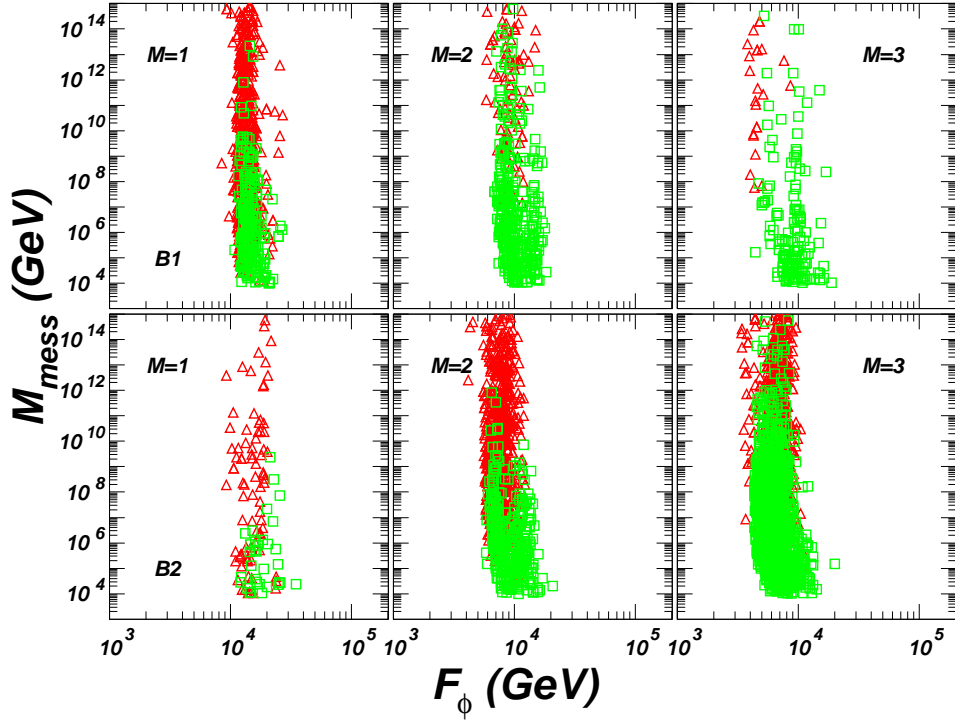


Figure 4. Scatter plots showing F_ϕ versus the messenger scale M_{mess} for Scenario B. All the points satisfy both the lower and upper bounds of dark matter relic density and collider constraints. The red \triangle (green \square) samples are excluded (allowed) by the gluino mass bound $m_{\tilde{g}} \geq 1.5$ TeV.

matter relic density are shown as green ' \square '. The numerical calculation indicates that the number of points which satisfy the dark matter relic density decreases with M in Scenario B1, but increases with M in Scenario B2. This can be understood from the mass ratio between the bino and the gluino with (the most favorite) large negative deflection parameter $d \sim -4$. For a gluino mass between 1.5 TeV and 3 TeV, the mass ratio should be adjusted to a proper value at $M_3 : M_1 \sim \mathcal{O}(10)$ to fully account for the dark matter relic density by decreasing (Scenario B1) or increasing (Scenario B2) the value of M . Bino dominated neutralino often leads to over-abundance of DM, unless (co)annihilation processes reduce the relic density to levels compatible with Planck.

We should note that some portion of the parameter space with insufficient DM relic abundance is not displayed in Fig.4 and Fig.5. Following the discussions in Scenario A, we obtain Table 2 from Eq.(3.7), showing the range of the deflection parameter d within which the wino is lighter than bino. Constrained by F_ϕ , a light wino-like DM will always lead to insufficient relic abundance.

The DM Spin-Independent(SI) direct detection constraints from LUX and PandaX are shown in Fig.6. It can be seen that a large portion of points that satisfy the DM relic density can survive the SI direct detection constraints. We know that interactions between bino DM and the nucleons are primarily mediated by t-channel scalar higgses (h_0 and H_0), or by s-channel squarks (with t-channel Z-boson exchange pro-

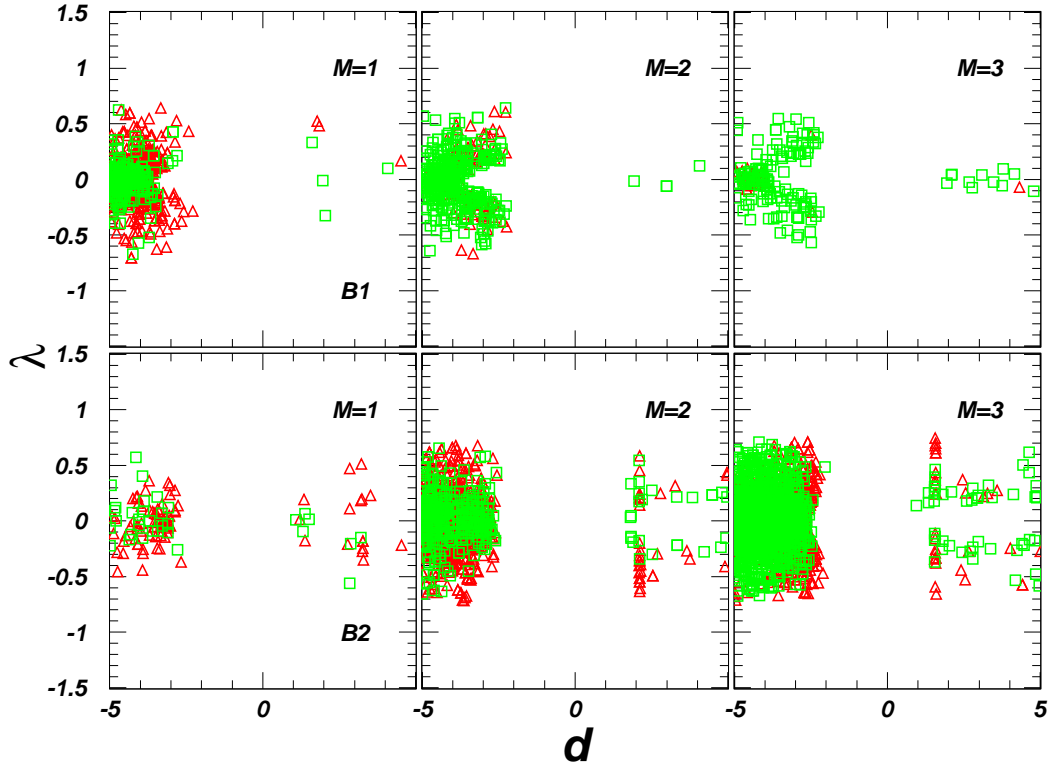


Figure 5. Same as Fig.4, but showing the deflection parameter d versus the messenger-matter couplings λ_E .

Table 2. The range of d within which the wino will be lighter than bino for various messenger species M in Scenario B.

		M=1	M=2	M=3
Scenario B1	d	$-0.92 \lesssim d \lesssim 1.23$	$-0.51 \lesssim d \lesssim 0.78$	$-0.35 \lesssim d \lesssim 0.95$
Scenario B2	d	$-1.21 \lesssim d \lesssim 1.05$	$-0.69 \lesssim d \lesssim 0.64$	$-0.49 \lesssim d \lesssim 0.46$

cess highly suppressed). As the squarks are not found at the LHC, their masses should be significantly larger than the higgs masses. So the SI cross section is dominated by higgs-mediated process, despite the associated suppression by yukawa couplings and the small higgsino fraction. In scenario B, the type of the neutralino which can give the right DM relic abundance is almost bino-like with small higgsino component, thus suppress the SI direct detection cross sections.

4 Conclusions

We proposed to introduce general messenger-matter interactions in the deflected anomaly mediated SUSY breaking scenario to explain the $g_\mu - 2$ anomaly. Scenarios with complete or incomplete GUT multiplet messengers were discussed, respectively. We found that the $g_\mu - 2$ anomaly can be solved in both scenarios under current constraints including the gluino mass bounds, while the scenarios with incomplete GUT representation messengers

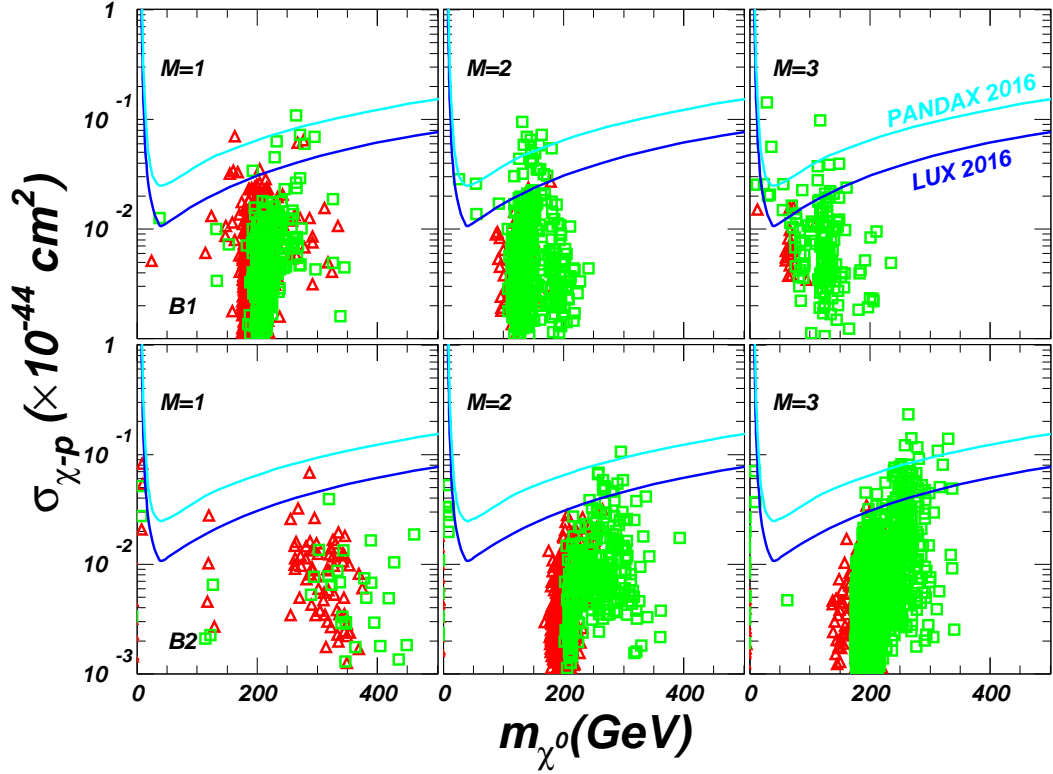


Figure 6. Same as Fig.4, but showing the Spin-Independent DM direct detection constraints from LUX 2016 and PandaX.

are more favored by the $g_\mu - 2$ data. We also found that the gluino is upper bounded by about 2.5 TeV (2.0 TeV) in Scenario A and 3.0 TeV (2.7 TeV) in Scenario B if the generalized deflected AMSB scenarios are used to fully account for the $g_\mu - 2$ anomaly at 3σ (2σ) level. Such a gluino should be accessible in this future LHC searches.

Acknowledgement

This work was supported by the Natural Science Foundation of China under grant numbers 11375001, 11675147, 11675242, by the Open Project Program of State Key Laboratory of Theoretical Physics, ITP, CAS (No.Y5KF121CJ1), by the Innovation Talent project of Henan Province under grant number 15HASTIT017 and the Young-Talent Foundation of Zhengzhou University, by the CAS Center for Excellence in Particle Physics (CCEPP), and by the CAS Key Research Program of Frontier Sciences.

References

- [1] G. Aad et al.(ATLAS Collaboration), Phys. Lett. B710, 49 (2012).
- [2] S. Chatrchyan et al.(CMS Collaboration), Phys. Lett.B710, 26 (2012).
- [3] The ATLAS collaboration, ATLAS-CONF-2016-052.
- [4] The ATLAS collaboration, ATLAS-CONF-2016-050.

- [5] M. Byrne, C. Kolda and J. E. Lennon, Phys. Rev. D **67**, 075004 (2003).
- [6] A. H. Chamseddine, R. L. Arnowitt and P. Nath, Phys. Rev. Lett. **49**, 970 (1982);
H. P. Nilles, Phys. Lett. B **115**, 193 (1982); L. E. Ibanez, Phys. Lett. B **118**, 73 (1982);
R. Barbieri, S. Ferrara and C. A. Savoy, Phys. Lett. B **119**, 343 (1982); H. P. Nilles,
M. Srednicki and D. Wyler, Phys. Lett. B **120**, 346 (1983); J. R. Ellis, D. V. Nanopoulos and
K. Tamvakis, Phys. Lett. B **121**, 123 (1983); J. R. Ellis, J. S. Hagelin, D. V. Nanopoulos and
K. Tamvakis, Phys. Lett. B **125**, 275 (1983); N. Ohta, Prog. Theor. Phys. **70** (1983) 542;
L. J. Hall, J. D. Lykken and S. Weinberg, Phys. Rev. D **27**, 2359 (1983).
- [7] M. Dine, W. Fischler and M. Srednicki, Nucl. Phys. B **189**, 575 (1981); S. Dimopoulos and
S. Raby, Nucl. Phys. B **192**, 353 (1981); M. Dine and W. Fischler, Phys. Lett. B **110**, 227
(1982); M. Dine and A. E. Nelson, Phys. Rev. **D48**, 1277 (1993); M. Dine, A. E. Nelson and
Y. Shirman, Phys. Rev. **D51**, 1362 (1995); M. Dine, A. E. Nelson, Y. Nir and Y. Shirman,
Phys. Rev. **D53**, 2658 (1996); G. F. Giudice and R. Rattazzi, Phys. Rept. **322**, 419 (1999).
- [8] L. Randall and R. Sundrum, Nucl. Phys. B **557**, 79 (1999); G. F. Giudice, M. A. Luty,
H. Murayama and R. Rattazzi, JHEP **9812**, 027 (1998).
- [9] I. Jack, D. R. T. Jones, Phys. Lett. B **465** (1999) 148.
- [10] I. Jack and D. R. T. Jones, Phys. Lett. B **482**, 167 (2000); E. Katz, Y. Shadmi and Y.
Shirman, JHEP **9908**, 015 (1999); N. ArkaniHamed, D. E. Kaplan, H. Murayama and Y.
Nomura, JHEP **0102**, 041 (2001); R. Sundrum, Phys. Rev. D **71**, 085003 (2005); K. Hsieh and
M. A. Luty, JHEP **0706**, 062 (2007); Y. Cai and M. A. Luty, JHEP **1012**, 037 (2010); T.
Kobayashi, Y. Nakai and M. Sakai, JHEP **1106**, 039 (2011).
- [11] A. Pomarol and R. Rattazzi, JHEP **9905**, 013 (1999); R. Rattazzi, A. Strumia, James D.
Wells, Nucl. Phys. B **576**, 3(2000).
- [12] N. Okada, Phys. Rev. D **65** (2002) 115009; N. Okada, H. M. Tran, Phys. Rev. D **87** (2013)
035024.
- [13] F. Wang, W. Wang, J. M. Yang and Y. Zhang, JHEP **1507**, 138 (2015) [arXiv:1505.02785
[hep-ph]].
- [14] F. Wang, Phys. Lett. B **751**, 402 (2015).
- [15] G.F. Giudice, R. Rattazzi, Nucl. Phys. B **511**:25-44(1998).
- [16] T. Han, T. Yanagida and R. J. Zhang, Phys. Rev. D **58**, 095011 (1998).
- [17] I. Gogoladze, A. Mustafayev, Q. Shafi, C. S. Un, Phys. Rev. D **94**, 075012 (2016); I.
Gogoladze, C. S. Un, Phys. Rev. D **95**, 035028 (2017).
- [18] L. Calibbi, T. Li, A. Mustafayev, S. Raza, Phys. Rev. D **93**, 115018 (2016).
- [19] G.F. Giudice, R. Rattazzi, Nucl. Phys. B **511**, 25 (1998).
- [20] J. A. Evans, David Shih, JHEP **08**, 093 (2013).
- [21] Z. Chacko and E. Ponton, Phys. Rev. D **66** (2002) 095004.
- [22] For a comparative study of NMSSM and MSSM, see, J. Cao *et. al.*, JHEP **1203**, 086 (2012)
[arXiv:1202.5821 [hep-ph]].
- [23] Y. Cai and M. A. Luty, JHEP **1012**, 037 (2010) [arXiv:1008.2024 [hep-ph]].
- [24] S. Schael et al. [ALEPH and DELPHI and L3 and OPAL and SLD and LEP Electroweak

Working Group and SLD Electroweak Group and SLD Heavy Flavour Group Collaborations], Phys. Rept. 427, 257 (2006) [hep-ex/0509008].

- [25] P. A. R. Ade et al. [Planck Collaboration], Astron. Astrophys. 571, A16 (2014).
- [26] J. Dunkley et al. [WMAP Collaboration], Astrophys. J. Suppl. 180, 306 (2009).
- [27] D. S. Akerib *et al.*, arXiv:1608.07648 [astro-ph.CO].
- [28] C. Fu et al., Spin-dependent WIMP-nucleon cross section limits from first data of PandaX-II experiment, Phys. Rev. Lett. 118, 071301 (2017)[arXiv:1611.06553].
- [29] V. Khachatryan et al. [CMS and LHCb Collaborations], Nature 522, 68 (2015);
- [30] C. Patrignani *et. al.* (Particle Data Group), Chin. Phys. C, **40** 100001 (2016).
- [31] M. Aaboud et al. [ATLAS Collaboration], Eur. Phys. J. C 76, 547 (2016); The CMS Collaboration, CMS-PAS-SUS-16-015; The ATLAS collaboration, ATLAS-CONF-2016-078; CMS Collaboration, CMS-PAS-SUS-16-030.